

## Article

# Insights from Biophotonic Imaging and Biochemical Analysis on Cellular and Molecular Alterations Exhibited in Dull Skin

Akira Matsubara <sup>1,\*</sup>, Tatsuya Omotezako <sup>2</sup>, Ying Xu <sup>2</sup>, Anna Evdokiou <sup>3</sup>, Lijuan Li <sup>3</sup>, Wenzhu Zhao <sup>3</sup>, Camila Pereira Braga <sup>3</sup>, Dionne Swift <sup>3</sup>, Hitomi Nagasawa <sup>1</sup>, Jennifer I. Byrd <sup>3</sup>, Brad Jarrold <sup>3</sup>, Gang Deng <sup>2</sup>, Junjie Wang <sup>4,5</sup> and Tomohiro Hakoziaki <sup>3</sup>

<sup>1</sup> Procter & Gamble Innovation G.K., 7-1-18 Onoedori, Chuo-ku, Kobe 651-0088, Hyogo, Japan; nagasawa.h@pg.com

<sup>2</sup> Procter & Gamble International Operations SA SG Branch, 70 Biopolis Street, Singapore 138547, Singapore; omotezako.t.1@pg.com (T.O.); xu.y.13@pg.com (Y.X.); deng.ga@pg.com (G.D.)

<sup>3</sup> The Procter & Gamble Company, Mason Business and Innovation Center, 8700 Mason Montgomery Road, Mason, OH 45040, USA; evdokiou.al.1@pg.com (A.E.); li.l.28@pg.com (L.L.); zhao.wh@pg.com (W.Z.); pereirabraga.c.1@pg.com (C.P.B.); swift.dp@pg.com (D.S.); byrd.ji@pg.com (J.I.B.); jarrold.bb@pg.com (B.J.); hakoziaki.t.1@pg.com (T.H.)

<sup>4</sup> Beijing Laboratory of Biomedical Imaging, Beijing Municipal Education Commission, Building 5 Hive Factory (East), No. 16 Anningzhuang East Road, Haidan District, Beijing 100085, China; junjie\_wang@pku.edu.cn

<sup>5</sup> National Biomedical Imaging Center, State Key Laboratory of Membrane Biology, Institute of Molecular Medicine, Peking-Tsinghua Center for Life Sciences, College of Future Technology, Peking University, No. 5 Yiheyuan Road, Haidan District, Beijing 100871, China

\* Correspondence: matsubara.a@pg.com; Tel.: +81-78-336-6022; Fax: +81-78-336-6171

**Abstract:** Dullness or lack of radiance in facial appearance is a common concern among females. Previous studies have linked skin dullness to aging and revealed alterations in skin pigments. However, younger individuals (ages  $\leq 35$ ) also report concerns about dull skin in their hectic daily lives, which may not involve pigmentation changes. We hypothesized that the mechanisms underlying dullness in youth differ from those associated with aging. To investigate this, we measured cellular and molecular changes in 132 healthy Japanese and Chinese females aged 18 to 35 using biophotonic multiphoton tomography and biochemical tape-strip analysis. Our findings revealed that dull skin exhibited a thicker stratum granulosum and less densely packed keratinocytes in deeper layers. Biochemical analysis showed upregulation of interleukin-36 $\gamma$  and downregulation of E-cadherin in dull skin, with interleukin-36 $\gamma$  levels negatively correlating ( $p = 0.023$ ) with metabolites of filaggrin. These alterations resemble those observed in inflammatory skin conditions, suggesting an additional mechanism of skin dullness beyond pigmentation. In vitro cultured cell models evaluated the efficacy of three skincare ingredients: galactomyces fermentation filtrate, bisabolol, and batyl alcohol. Galactomyces suppressed interleukin-36 $\gamma$  ( $p = 0.037$ ), while both batyl alcohol ( $p = 0.006$ ) and bisabolol ( $p = 0.049$ ) showed beneficial effects on filaggrin. Targeting these biomarkers may improve the appearance of dull skin.

**Keywords:** skin radiance; skin dullness; interleukin-36 $\gamma$ ; E-cadherin; filaggrin; galactomyces fermentation filtrate; bisabolol; batyl alcohol; biophotonics; biochemistry



**Citation:** Matsubara, A.; Omotezako, T.; Xu, Y.; Evdokiou, A.; Li, L.; Zhao, W.; Braga, C.P.; Swift, D.; Nagasawa, H.; Byrd, J.I.; et al. Insights from Biophotonic Imaging and Biochemical Analysis on Cellular and Molecular Alterations Exhibited in Dull Skin. *Cosmetics* **2024**, *11*, 219. <https://doi.org/10.3390/cosmetics11060219>

Academic Editor: Paolo Mariani

Received: 17 October 2024

Revised: 4 December 2024

Accepted: 8 December 2024

Published: 12 December 2024



**Copyright:** © 2024 by the authors. Licensee MDPI, Basel, Switzerland. This article is an open access article distributed under the terms and conditions of the Creative Commons Attribution (CC BY) license (<https://creativecommons.org/licenses/by/4.0/>).

## 1. Introduction

Dull skin is a common concern among females, often characterized by lack of radiance. “Dull” and “radiant” are terms that are frequently used in everyday conversation, and these terms are defined as the dark and bright aspect of an object by dictionaries. Therefore, in past research, radiant skin has been often defined as having a brighter and lighter tone with a healthy glow, while dull skin is characterized by a darker tone and a lack of energy

or tired appearance, and these optical characteristics and skin features have been the focus of numerous investigations [1–13].

The reflection of light from the deeper layers of the skin is significantly influenced by the absorption of the incident light by skin pigments such as melanin and bilirubin [2]. Surface reflection, on the other hand, is affected by the skin's roughness. A smoother surface, which is generally characteristic of youthful skin, gives a healthy glow [3]. The homogeneity of skin complexion and the surface roughness of the skin play crucial roles in overall skin radiance, which in turn influences facial attractiveness, as well as the perception of age and health [4,5]. As a result, the cosmetics industry has a significant interest in understanding skin dullness to help consumers in achieving more radiant skin through skincare treatments [6,7].

Previous studies have characterized dull or radiant skin as an aging issue, as many females perceive their skin to be more radiant at a younger age, with this radiance diminishing over time. Indeed, changes in skin complexion and texture occur alongside chronological aging [8]. As a result, the issue of dull skin has often been considered a part of the aging process, leading to research on a lack of radiance associated with aging [9–13]. These studies have focused on different age groups to understand the differences between younger and older individuals. In 1997, Kaneko et al. examined the relationship between aging and changes in skin surface properties and concluded that roughness and transparency on top of melanin and blood circulation are associated with skin dullness [9,10]. In 2007, Petitjean et al. proposed a novel method for evaluating skin radiance by measuring light reflection characteristics using the bidirectional reflection distribution function (BRDF) [11]. They compared a radiant skin group ( $n = 15$ , average age = 31) with a dull skin group ( $n = 15$ , average age = 41). More recently, Nurani et al. (2023) reported that skin dullness can be defined using colorimetric, optical, and skin surface microtopography parameters, with the perception of dullness increasing with chronological age [12]. Lua et al. (2024) studied the association between skin yellowness and the perception of dullness or radiance among 185 Chinese females aged 20 to 49, analyzing changes across age groups [13]. These historical studies consistently reveal that dull or radiant skin is not a singular attribute but a combination of multiple skin features, particularly in relation to skin tone residing in skin pigments. However, there is less research that targets the cellular or molecular aspect of dull and radiant skin other than pigments. In 2011, Kawabata et al. reported that N $\epsilon$ -(carboxymethyl) lysine, known as an advanced glycation end product (AGE), is formed with aging and contributes to a yellowish skin tone, a symptom of dullness [14]. In 2020, Laughlin et al. studied 150 Chinese females (ages 20–50) and collected skin biopsies, revealing that AGEs are present in aged dull skin and that *in vitro* activation of autophagy can reduce AGEs in keratinocytes, potentially improving skin dullness [15]. These studies address the mechanisms of skin dullness at a molecular level, yet dull skin is associated with aging.

Contemporary females report experiencing skin dullness during particularly hectic periods of their lives, such as during times of insufficient sleep or high stress [16,17]. This suggests that skin dullness is not solely a long-term issue associated with aging; it also represents a short-term problem that affects their skin of today. Younger generations, particularly those under age 35, who have not yet begun to experience noticeable signs of skin aging, are particularly motivated to maintain their youthful skin appearance during busy times. Lack of sleep or stress can induce various reactions such as inflammation [18,19] that damages the skin cells, and as skin pigment alterations would not happen in such a short time, we hypothesized that differing mechanisms from well-known root causes are contributing to the dull skin. To our best knowledge, there is little prior research that focuses on the skin dullness in the aging context and studied its underlying mechanism.

Therefore, our study aimed to explore the potential mechanisms of skin dullness among younger individuals in terms of cellular and molecular alterations. For the cellular alterations, we utilized biophotonic multiphoton tomography (MPT), as we can observe the structures of cells non-invasively. For the molecular alterations, biochemical composition

analysis was conducted via tape stripping. While we can obtain limited information from tape strips, we aimed at better understanding the underlying mechanism of dull and radiant skin by analyzing proteins in stratum corneum layers from tape-stripping samples. Through these approaches, we sought to identify new mechanisms of skin dullness. In addition, we aimed to assess whether skin dullness could be addressed through skincare materials for future opportunities.

## 2. Materials and Methods

Our study consists of three components: two skin studies aimed at understanding the difference between radiant and dull skin and an evaluation of skincare materials in 2D/3D skin models. In the first skin study, we investigated the structural difference between radiant and dull skin utilizing multi-photon tomography (MPT). In the second skin study, we explored the molecular mechanisms underlying these structural differences by collecting tape-strip samples from the skin and analyzing them for biomarkers. Finally, we evaluated the efficacy of skincare materials in 2D and 3D skin models to explore potential skincare interventions.

### 2.1. Skin Study #1

#### 2.1.1. Overall Design of Skin Study #1

Eleven Chinese females with generally healthy skin participated in the first study. Prior to commencing the study and collecting data, we obtained institutional review board approval for the study protocols from the Ethics Committee of Cosmetics Technology Center, Chinese Academy of Inspection and Quarantine, Beijing, China (IRB number: 2023-008-DY-192). This was a small exploratory study aimed at determining whether we can find any difference between radiant and dull skin at the cellular level. The age range of the subjects was 18 to 35 years old, with mean  $\pm$  standard deviation of  $24.2 \pm 5.2$  years. We utilized MPTflex™ (JenLab GmbH, Berlin, Germany) to obtain preliminary findings on the differences at the cellular level [20]. Additionally, we captured facial images of the subjects using a Dynamic Tone Imaging System (DTIS, a custom-made imaging system) to collect facial skin images for visual grading to determine whether the skin is relatively radiant or dull.

#### 2.1.2. Multi-Photon Tomography (MPT) and Image Analysis of Cell Nuclei

The MPTflex™ system is based on a Ti:Sapphire femtosecond laser for in vivo imaging, with a scanning field of view of approximately  $245 \times 245 \mu\text{m}$  and imaging depth  $\geq 200 \mu\text{m}$  (resolutions of  $<0.5 \mu\text{m}$  laterally and  $<2 \mu\text{m}$  axially). MPT measurement offers sub-micron resolution with two optical channels: two-photon excited autofluorescence (AF) detects epidermal cells and elastic fibers, and second harmonic generation (SHG) detects non-linear structures such as collagen fibers. For each subject, we performed three MPT measurements from adjacent areas on the left cheek at  $2.5 \mu\text{m}$  z-steps from  $0 \mu\text{m}$  to  $200 \mu\text{m}$ , resulting in three 3D-xyz images (z-stacks of 81 en face AF/SHG images with  $512 \times 512$  pixels). The captured images were processed and analyzed for epidermal cell nucleus count. As each xy image had a dark fringe in the surrounding area, and all images from the start to end slices were cropped from the center to  $282 \times 282$  pixels for noise removal. Then, for each image, the nuclei were segmented and detected by initially applying a median filter to preserve the edge, followed by the 2D Hessian blob detection algorithm [21]. The three sets of data from each individual subject were averaged for further statistical analysis. All image processing, segmentation, and analysis were implemented in Matlab 2022b (MathWorks Inc., Natick, MA, USA).

### 2.2. Skin Study #2

#### 2.2.1. Overall Design of Skin Study #2

One hundred twenty-one Japanese females with generally healthy skin participated in the second study. Prior to commencing the study and collecting data, we obtained

institutional review board approval for the study protocols from the Ethical Review Board of Interface Inc., Akita, Japan (IRB number: 21000027). The age range of the subjects was 20 to 35 years old, with mean  $\pm$  standard deviation of  $27.3 \pm 4.9$  years. Facial skin images were captured using the DTIS for visual grading, and VISIA-CR<sup>®</sup> (Canfield Scientific, Parsippany, NJ, USA) [22] was used for computerized skin image analysis following previously reported methods [23–27]. TEWL was also measured on the cheek where the images were captured using VapoMeter<sup>®</sup> (Delfin Technologies Ltd., Kuopio, Finland) [28]. In addition to the instrumental measurements, tape stripping was performed on the cheek using D-Squame<sup>®</sup> adhesive discs (Clinical and Derm, Dallas, TX, USA). The tape strips were applied to the skin, pressed using the designated pressure device, and then carefully removed to collect the stratum corneum. Each subject underwent the application of a series of five consecutive tape strips on the same area to ensure sufficient sample collection. The collected tape strips were immediately placed in a dry ice box and stored at  $-80$  °C until further analysis. The samples were later analyzed for biomarkers using liquid chromatography coupled with tandem mass spectrometry (LC-MS/MS) [29].

### 2.2.2. DTIS and Visual Grading for Skin Dullness and Radiance

The DTIS is a custom-made imaging system designed to capture facial skin images under controlled and evenly illuminated light conditions. Three flat LED light panels are positioned in the front left, front right, and bottom positions to illuminate the subject's face from multiple angles (Figure 1). The lighting illuminates the entire face and is optimized to view the cheeks, an area of particular concern for many females regarding the presence or absence of radiance. The system incorporates a digital camera, EOS Kiss x10i (Canon Inc., Tokyo, Japan), which enables the digital recording of facial images, with an EF-S 60 mm F2.8 macro lens (Canon Inc.). These captured images are then displayed on a color-calibrated LCD monitor (ColorEdge CG2420; EIZO Corporation, Hakusan, Japan) for visual grading. To maintain consistent and accurate assessment conditions, the visual grading was conducted in a dark room, eliminating any external or room light interference.

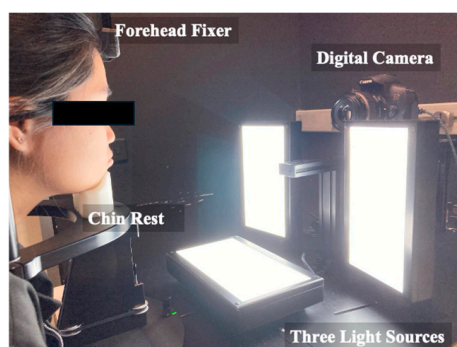


**Figure 1.** An overview of the DTIS. This is a custom-made facial imaging system to capture facial skin appearance under controlled and even illumination, and the images were utilized for the visual grading of radiance or dullness.

During the visual grading process, the facial images were presented individually at the center of the monitor, accompanied by questions relating to the perception of skin radiance. Untrained female respondents provided their assessments based on their own perceptions. In the first study, visual grading was conducted by 10 respondents, while in the second study, it involved 117 respondents. The grading was conducted on a 10-point scale where a rating of 1 is the most dull and 10 is the most radiant appearance, as judged subjectively by the grader. The scores obtained from multiple respondents were averaged, and based on these scores, the radiance (or dullness) scores of individual subjects were determined.

### 2.2.3. Biochemical Composition Analysis from Tape-Strip Samples

#### IL-36 $\gamma$ Assay

Stratum corneum (SC) specimens were collected from each participant and analyzed for a target panel of SC proteins through their unique peptides using ultra-performance liquid chromatography coupled with tandem mass spectrometry (UPLC-MS/MS). Two SC tape strips were extracted with 1.5 mL of 50 mM ammonium bicarbonate (ABC) buffer containing heavy peptide standards. A 50  $\mu$ L aliquot of the extract was dried down and reconstituted with mobile phase A for protein analysis using bicinchoninic acid (BCA) assay (Thermo Scientific, Rockford, IL, USA) and bovine serum albumin as standard. The rest of the extract was dried down and reconstituted with ABC buffer for subsequent reduction, alkylation, and digestion with trypsin/LysC. The digest was then dried and reconstituted in 50  $\mu$ L of 0.1% formic acid in water for analysis. The target light peptides and corresponding heavy peptides were separated on a Waters Acquity Premium Peptide BEH C18 column (2.1  $\times$  100 mm, 1.7  $\mu$ m particles; Waters, Milford, MA, USA). Mobile phase A was 0.1% formic acid in water and mobile phase B was 0.1% formic acid in acetonitrile. Detection was performed by tandem mass spectrometry (AB Sciex 7500; Sciex, Framingham, MA, USA) operating under multiple reaction monitoring (MRM) conditions and positive electrospray ionization mode (ESI+). Relative quantitation of each protein was performed from its corresponding peak area ratio of light peptide to heavy peptide using Skyline (MacCoss Lab Software, Seattle, WA, USA). The quantitation was then normalized by BCA protein to account for the protein content in each extract.

#### Filaggrin Metabolite Assay

Stratum corneum (SC) specimens were collected from each participant and analyzed for 2-pyrrolidone-5-carboxylic acid (PCA), and cis- and trans-urocanic acid (UCA), which are major metabolites of filaggrin (FLG), using ion-pairing reverse-phase liquid chromatography coupled with tandem mass spectrometry (IP-RPLC-MS/MS). Two SC tape strips were extracted with 1.5 mL of mobile phase A (0.1% formic acid and 0.1% heptafluorobutyric acid in water). To create a parent plate for analysis, 200  $\mu$ L of each extract was combined with 45  $\mu$ L of internal standard solution (2-pyrrolidone-5-carboxylic acid (3,3,4,4,5-D<sub>5</sub>); cis-urocanic acid (1,2,3-<sup>13</sup>C<sub>3</sub>)) and 800  $\mu$ L of mobile phase A in a 96-well plate. Subsequently, the injection plate was created by transferring 50  $\mu$ L from each well of the parent plate to analogous wells of a daughter plate and then adding 450  $\mu$ L of mobile phase A across all wells. The analytes and internal standards were separated on a Waters Atlantis T3 column (2.1  $\times$  100 mm, 3  $\mu$ m particles; Waters, Milford, MA, USA). Mobile phase B was 0.1% formic acid and 0.1% heptafluorobutyric acid in acetonitrile. Detection and quantitation were performed by tandem mass spectrometry (AB Sciex 6500; Sciex, Framingham) operating under multiple reaction monitoring (MRM) conditions and positive electrospray ionization mode (ESI+). The concentration of PCA and UCA in the study specimens was determined from the corresponding peak area ratio by interpolation from the regression curve of calibration standards. The nominal range of quantitation was 20 to 20,000 ng/mL. The concentration of PCA and UCA determined in the extracts was corrected for its dilution factor and then normalized by BCA protein concentration in the same extract.

#### E-Cadherin (CDH1) Assay

Stratum corneum (SC) specimens were collected from each subject and analyzed using a label-free quantification proteomic approach. Briefly, two tape strips were extracted with 300  $\mu$ L of 100 mM ABC buffer (pH 8.0) three times and then 300  $\mu$ L of 80% methanol (MeOH). With the aid of MeOH and chloroform, each extract separated into three portions, namely, polar metabolites, lipids, and proteins. Proteins were precipitated in cold acetone (−20 °C) and centrifuged to a pellet at 14,000 $\times$  *g*. The pellets were further rinsed with cold acetone prior to enzymatic digestion. For protein digestion, the pellets were first reconstituted with denaturation buffer (50 mM ABC, pH 8.5; 10 mM Tris (2-carboxyethyl) phosphine (TCEP); 5% sodium deoxycholate) at 60 °C for 10 min, and then alkylated with

alkylation solution (100 mM iodoacetamide) at room temperature for 60 min in the dark. Following alkylation, proteins were digested with trypsin solution (1 µg/µL) at 37 °C overnight in the dark and then quenched with 10% trifluoroacetic acid (TFA). The digested samples were centrifuged at 15,000× *g* to pellet sodium deoxycholate. The supernatants were analyzed on an LC-TIMS-MS/MS platform (Bruker Daltonics, Bremen, Germany) including a nanoElute UHPLC system coupled to a timsTOF Flex mass spectrometer equipped with a CaptiveSpray ion source. Tryptic peptides were separated on a PrepSep C18 nanocolumn (0.15 × 250 mm, 1.5 µm particles; Bruker Daltonics) using a linear gradient between 0.1% formic acid in water and 0.1% formic acid in acetonitrile at 55 °C. Raw MS data were processed using MaxQuant (Cox Lab Software; Max Planck Institute of Biochemistry, Martinsried, Germany) and the generated MS/MS spectra were used as search queries in the UniProt human database.

### 2.3. Skincare Material Testing in 2D/3D Skin Models

We tested three skincare materials in four experiments, as summarized in Table 1.

**Table 1.** Summary of cultured cell experiments. Four skincare materials were evaluated for the effects on IL-36γ, CDH1, and FLG in 2D/3D skin models.

| Experiment No.<br>(Sample Size,<br>Treatment Duration) | Cultured<br>Cell Tissue | Treatment   | Concentration                      | Manufacturer   | Endpoint |
|--|-------------------------|---|------------------------------------|--|----------|
| 1<br>( <i>n</i> = 3, 24 h)                             | 2D HEK <sub>n</sub> *   | Vehicle (DMSO **)<br>GFF ***<br>Batyl alcohol       | 0.1%<br>5.0%<br>0.25%              | Sigma Aldrich<br>P&G IGK<br>Sigma Aldrich            | IL-36γ   |
| 2<br>( <i>n</i> = 4, 24 h)                             | 2D HEK <sub>n</sub>     | Vehicle (DMSO)<br>Bisabolol                         | 0.1%<br>0.000625%                  | Sigma Aldrich<br>Symrise                             | IL-36γ   |
| 3<br>( <i>n</i> = 4, 24 h)                             | 2D HEK <sub>n</sub>     | Vehicle (DMSO)<br>GFF<br>Bisabolol<br>Batyl alcohol | 0.1%<br>5.0%<br>0.000625%<br>0.25% | Sigma Aldrich<br>P&G IGK<br>Symrise<br>Sigma Aldrich | CDH1     |
| 4<br>( <i>n</i> = 6, 5 days)                           | 3D skin equivalent      | Vehicle (DMSO)<br>GFF<br>Bisabolol<br>Batyl alcohol | 0.1%<br>10.0%<br>0.005%<br>0.25%   | Sigma Aldrich<br>P&G IGK<br>Symrise<br>Sigma Aldrich | FLG      |

\* normal human epidermal keratinocyte (HEK<sub>n</sub>), \*\* dimethyl sulfoxide (DMSO), \*\*\* galactomyces fermentation filtrate (GFF).

#### 2.3.1. Keratinocyte Culture

Cell culture media and supplements including EpiLife with gentamicin/amphotericin B, human keratinocyte growth supplement (HKGS), HKGS kit, trypsin/EDTA solution, trypsin neutralizer solution, penicillin/streptomycin (10,000 U/mL, 100×), and DPBS were purchased from Thermo Fisher Scientific (Waltham, MA, USA). Human neonatal epidermal keratinocytes (HEK<sub>n</sub>, Cascade Biologics Inc, Portland, OR, USA, Cat#: C-001-5C, Lot: 1C0313) were expanded in a 5% CO<sub>2</sub>, 37 °C incubator using EpiLife medium with HKGS and gentamicin/amphotericin B. The HEK<sub>n</sub> cells used in these experiments had not been passaged more than five times. When treating the cells, starvation medium containing gentamicin/amphotericin B, bovine insulin, bovine transferrin, and hydrocortisone was used. HEK<sub>n</sub> cells were seeded into six-well plates at a density of 1 × 10<sup>5</sup>, allowed to grow to 70% confluence, and then treated for 24 h with galactomyces fermentation filtrate (GFF) (P&G Innovation G.K., Kobe, Japan), batyl alcohol (Sigma Aldrich, St. Louis, MO, USA), or bisabolol (Symrise, Teterboro, NJ, USA).

### 2.3.2. Protein Extraction

For protein extraction, radioimmunoprecipitation assay (RIPA) buffer (Thermo Fisher Scientific, Waltham, MA, USA) was supplemented with Halt (Invitrogen, Carlsbad, CA, USA) protease and phosphatase inhibitor cocktails and added to cells after rinsing with DPBS. Cells were sonicated on ice in a Branson (Model CPX3800H; Emerson, Danbury, CT, USA) sonicating water bath for 60 min. Lysates were centrifuged at  $14,000\times g$  for 15 min at 4 °C. After centrifugation, the supernatant was collected in a fresh Eppendorf tube, placed on ice, and then aliquoted for storage at  $-80\text{ }^{\circ}\text{C}$ . Quantification of total protein was accomplished using a BCA assay (Pierce, Waltham, MA, USA) and a SpectraMax 250 Microplate Reader on the analytical software SoftMax Pro V3.1.1.

### 2.3.3. Skin Equivalent Culture

A 3D human epidermal skin organotypic model (Epi-100; MatTek Corporation, Ashland, MA, USA) was used to investigate the effects of skincare materials, including bisabolol (Symrise, Teterboro, NJ) and GFF (P&G Innovation G.K., Kobe, Japan), compared with DMSO as a vehicle (Sigma Aldrich, St. Louis, MO, USA). Briefly, epidermal cultures ( $n = 6$  per treatment) were allowed to acclimate overnight in Dulbecco's modified Eagle's medium with epidermal growth factor, insulin, hydrocortisone, and proprietary stimulators of epidermal differentiation supplemented with gentamicin/amphotericin B at 37 °C in 5% CO<sub>2</sub>. Cultures were then treated by evenly spreading 10  $\mu\text{L}$  of each treatment mixture topically with a sterilized glass rod. Cultures were rinsed with Dulbecco's phosphate-buffered saline (DPBS) (MatTek Corporation) and provided with fresh culture medium upon daily treatment every 24 h for 5 days. Upon the conclusion of the treatment period, each culture was rinsed in DPBS and bisected with a clean razor blade. Half of each culture was flash-frozen in liquid nitrogen for future analysis. The other half was embedded in optimum cutting temperature (OCT) compound (Sakura Finetek, Torrance, CA, USA) before freezing over liquid nitrogen and stored at  $-80\text{ }^{\circ}\text{C}$  until cryostat sectioning at 10  $\mu\text{m}$  thickness.

### 2.3.4. Histology and FLG Staining

The overall structural morphology and health of each culture were assessed by hematoxylin and eosin staining of 10  $\mu\text{m}$  frozen sections. Immunohistological assessment of FLG was performed using an optimized general protocol as previously described [30] and applying an anti-human FLG antibody (PA5-115235, 1:1000; Invitrogen, Waltham, MA, USA). In brief, 10  $\mu\text{m}$  frozen sections were fixed in 4% formaldehyde in PBS (Invitrogen, Waltham, MA, USA) before being blocked with 10% normal goat serum in PBS for 1 h at room temperature, then incubated overnight with anti-FLG antibody at 4 °C in a humidified chamber. A negative control section was incubated with only PBS. Sections were then washed and incubated with secondary goat anti-rabbit polyclonal antibody (150086, 1:1000; Abcam, Waltham, MA, USA) for 1 h at room temperature. For nuclear counterstaining, sections were incubated for 15 min with NucBlue fixed cell stain ReadyProbes reagent (Thermo Fisher Scientific, Waltham, MA, USA) before being coverslipped with mounting medium (Ibidi USA Inc., Fitchburg, WI, USA). For comparisons between treatments, three different 10 $\times$  field-of-view fluorescent images were captured for each culture with a Zeiss Observer Z1 microscope (Carl Zeiss Microimaging, White Plains, NY, USA) at the same gamma values, pixel range, and exposure.

Image Pro 10™ (Media Cybernetics, Rockville, MD, USA) image analysis software was used to segment the viable epidermis space beneath the bottom of the stratum corneum and above the culture well membrane. Within this viable epidermal space, the FLG-positive cellular area was quantified relative to the DAPI-positive cellular area. To account for differences in total cell number, the results are presented as the ratio of red (FLG) to blue (nuclei) signal. Statistical comparisons were performed using Student's *t*-test, where  $p < 0.05$  was considered to reflect a significant difference.

### 2.3.5. Enzyme-Linked Immunosorbent Assay

IL-36 $\gamma$  and CDH1 enzyme-linked immunosorbent assay (ELISA) kits were purchased from Abcam (267633 and 233611). Equal concentrations of total protein extracts from 2D monolayers cultured with treatment mixtures collected 24 h after treatment were applied to the ELISA plates. ELISAs were performed in accordance with the manufacturer's instructions and read using a SpectraMax 250 Microplate Reader on SoftMax Pro V3.1.1. Quantitative analysis of samples was performed in accordance with the manufacturer's recommendations.

### 2.4. Statistical Analysis

We performed all statistical analyses using JMP<sup>®</sup> Pro 18.0.1 (JMP Statistical Discovery LLC, Cary, NC, USA). The group comparison was performed by fitting the standard least squares model, and the marginal estimated means were examined for statistical significance using a *t*-test. For biochemical components, the distribution of the parameter was examined by using a Shapiro–Wilk test and, if the data were found to be non-normally distributed, log<sub>2</sub> transformation was applied to the data before statistical analysis. Throughout all of the analyses, a *p*-value of <0.05 was considered to indicate statistical significance.

## 3. Results

### 3.1. Differences at the Cellular Level Between Radiant and Dull Skin via MPT Measurement

The DTIS images were graded by 10 untrained respondents on a 10-point scale. Based on the obtained results, we allocated the subjects into groups with more radiant or duller skin (Figure 2). As such, six subjects were assigned to the more radiant skin group (mean score  $\pm$  SD = 6.74  $\pm$  0.48) and five to the duller skin group (mean score  $\pm$  SD = 4.88  $\pm$  0.41). The mean age of the radiant skin group was 24.5  $\pm$  2.2 years, while that of the dull skin group was 23.8  $\pm$  2.4 years, which did not differ significantly.

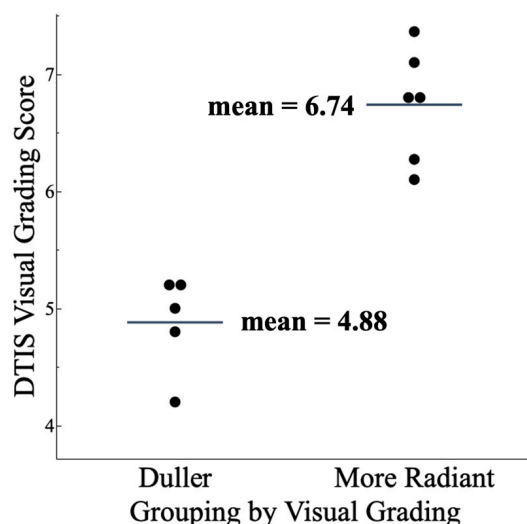


**Figure 2.** Skin radiance/dullness grouping by visual grading. Ten untrained respondents performed the visual grading using DTIS images displayed on a color-calibrated monitor. The grading was conducted on a 10-point scale, where a higher score indicated greater radiance. In this figure, each point represents an individual subject (a person in the image), and the threshold between the two groups was the median score of the 11 subjects.

### 3.2. Duller Skin Exhibits Altered Cornification Process

Prior to further analysis using MPT images, the images were visually examined by three scientists at Procter & Gamble. Based on their analysis, four boundaries in the skin layers were identified (Figure 3). Using these identified boundaries, we defined the layers between points A and B in Figure 3 as stratum granulosum because the process

of cornification of keratinocytes into corneocytes was observed in these layers. We then calculated the thickness of the stratum granulosum as the number of layers between these two points. Additionally, we calculated the thickness of the rest of the epidermis, which was defined as the number of layers between point B and the intermediate layer between points C and D. This approach was selected because the bottom of the epidermis (basal layer) was undulating, making it challenging to accurately determine the top and bottom layers. The results demonstrated that dull skin exhibited a significantly thicker stratum granulosum than radiant skin ( $p$ -value = 0.036), as shown in Figure 4a. On the other hand, no significant difference was found in the thickness of the remaining bottom layers of epidermis (Figure 4b). The thicker stratum granulosum in dull skin suggests alteration in the cornification process.

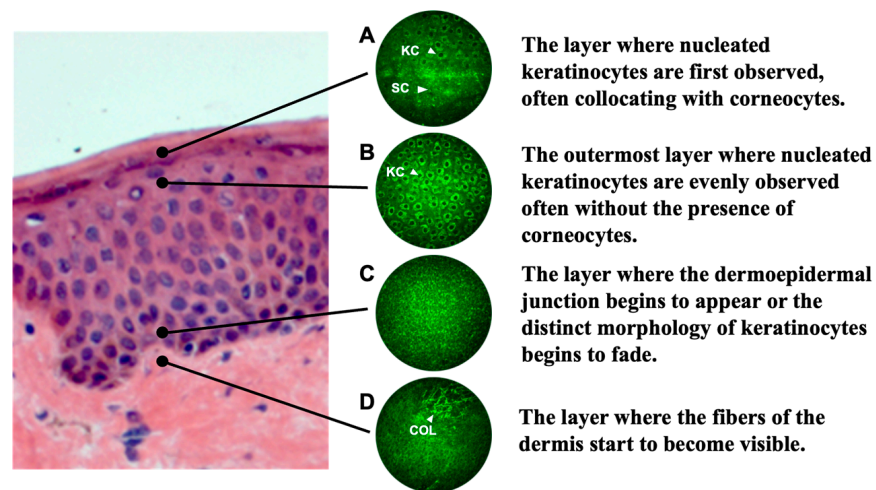


**Figure 3.** Determination of the skin layer boundaries. The skin layer boundaries were determined based on visual examination of the MPT images. We identified four boundaries of the skin layers as depicted in the figure. Between points A and B, keratinocytes are denucleated and are cornified. We define these layers as the stratum granulosum in this article. The bottom of the epidermis is difficult to identify, so we defined it as the point intermediate between points C and D. Abbreviations: keratinocyte (KC), stratum corneum (SC), collagen (COL).

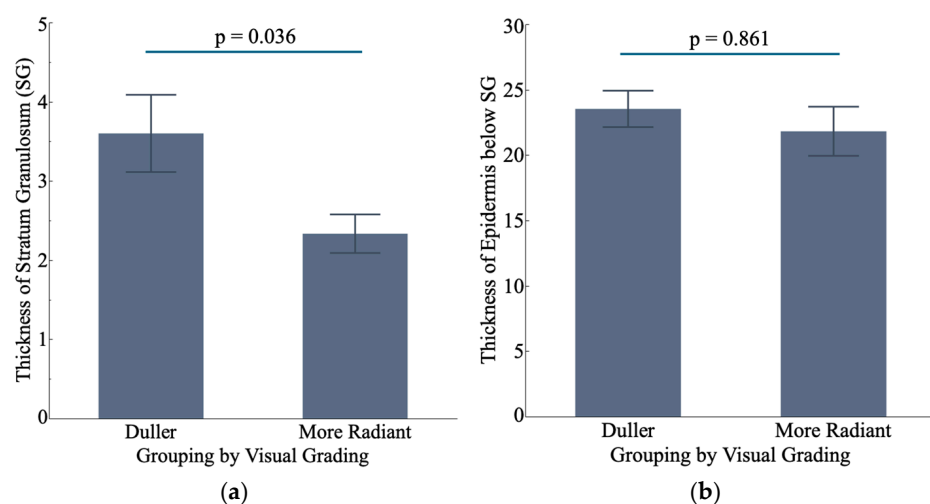


**Figure 4.** The thickness of skin layers. (a) Stratum granulosum (SG) and (b) the rest of the epidermis. The duller skin group ( $n = 5$ ) and the more radiant skin group ( $n = 6$ ) were determined by visual grading as described in Figure 2. In this measurement, one layer is equivalent to a thickness of 2.5  $\mu$ m.

### 3.3. Keratinocytes Are Less Densely Packed in Dull Skin than in Radiant Skin

Figure 5 presents the number of keratinocyte nuclei detected by MPT image analysis. The number of layers in Figure 5 is normalized from point B in Figure 3. Our data showed that more nuclei, and hence more keratinocytes, are present in radiant skin at the deeper region of the epidermis than in dull skin, with statistically significant differences observed in multiple layers, particularly between the 12th and 18th layers. This could indicate that keratinocytes at deeper layers are more tightly packed in radiant skin than in dull skin.

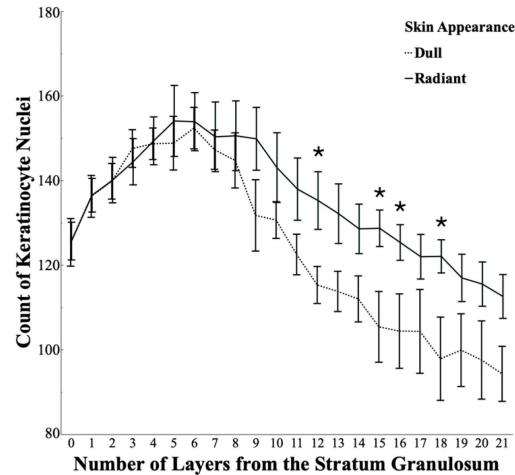


**Figure 5.** The count of nuclei of keratinocytes. The nuclei of keratinocytes were observed using MPT imaging. Layer 0 corresponds to point B defined in Figure 3, representing the bottom of the stratum granulosum layer. In this measurement, one layer is equivalent to a thickness of 2.5  $\mu\text{m}$ . The asterisks(\*) in the Figure indicate that the count of nuclei of radiant skin is statistically higher ( $p < 0.05$ ) than that of dull skin.

### 3.4. Molecular Differences Between Radiant and Dull Skin via Biochemical Analysis

#### 3.4.1. Lower IL-36 $\gamma$ and Higher CDH1 Were Found in Radiant Skin

We examined the biochemical compositions of the samples on the tape strips and analyzed their correlation to the radiance visual grading score. The results revealed a lower level of IL-36 $\gamma$ , which is reported as a marker of psoriatic skin, and a higher level of CDH1, which maintains the adhesive properties of junctions in keratinocytes and supports proper skin differentiation, among individuals with radiant skin (Figure 6).

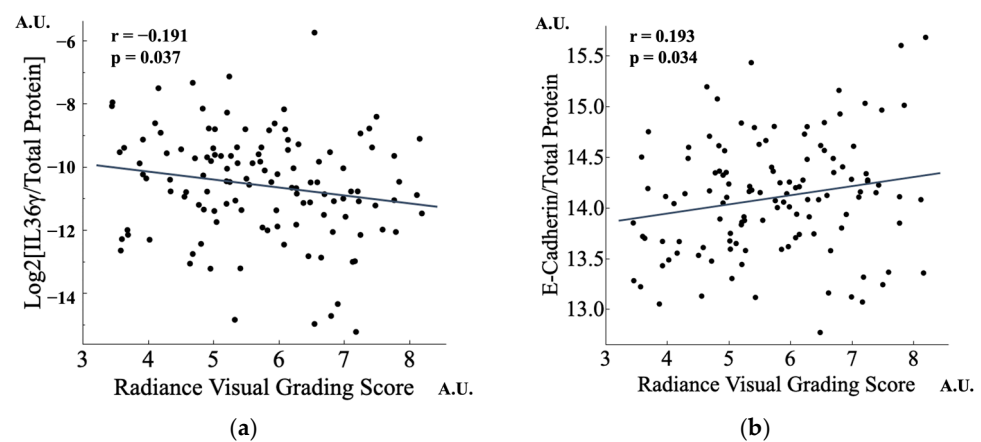


**Figure 6.** Correlation between biomarkers and skin radiance. (a) IL-36 $\gamma$  and (b) CDH1. Radiance skin score was determined by visual grading.

### 3.4.2. FLG Metabolites and IL-36 $\gamma$ Were Negatively Correlated

To investigate the relationship between IL-36 $\gamma$  and FLG metabolism, we measured major FLG metabolites, PCA, and cis- and trans-UCA, from SC tape strips and analyzed their correlations with IL-36 $\gamma$  levels (Figure 7). Cis-UCA is known to be produced from trans-UCA in the skin upon UV exposure, so the levels of these two complementary amino acids were added to obtain total UCA (hereafter simply referred to as “UCA”) for further statistical analysis. The results indicated that the FLG level in the skin could be reduced by the presence of IL-36 $\gamma$ , as often seen in psoriatic skin.

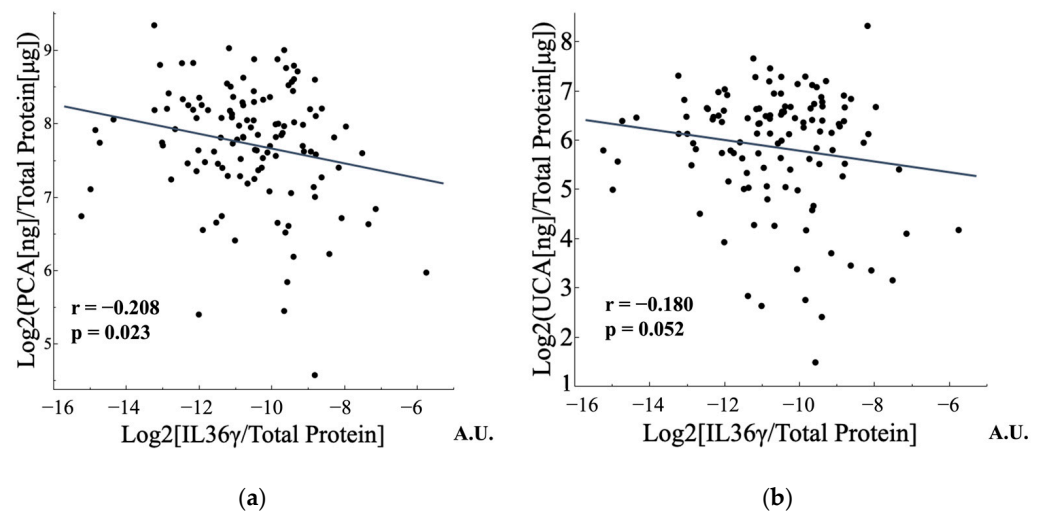


**Figure 7.** Correlations between IL-36 $\gamma$  and (a) PCA and (b) UCA. PCA and UCA are known metabolites of FLG. IL-36 $\gamma$  is known to be associated with psoriasis, in which the downregulation of FLG is observed. To determine whether the same pattern is seen in dull skin, we examined the correlation between IL-36 $\gamma$  and amino acids that are metabolites of FLG.

### 3.4.3. IL-36 $\gamma$ Is Also Potentially Associated with Changes in Skin Condition

The associations between IL-36 $\gamma$  levels and skin-surface-related parameters were examined. Prior to this analysis, we assigned the subjects to the high-IL-36 $\gamma$  group ( $n = 60$ ) and the low-IL-36 $\gamma$  group ( $n = 61$ ) using the median of IL-36 $\gamma$ /total protein levels as a threshold. These two groups were confirmed to show a significant difference in the level of IL-36 $\gamma$  (Figure 8a). We then examined the difference in skin parameters between these two groups. The results showed that the level of IL-36 $\gamma$  expression in the skin could impact the skin surface conditions such as TEWL (Figure 8b), skin redness (Figure 8c), and skin roughness (Figure 8d). This in turn suggests that IL-36 $\gamma$  may similarly disrupt the homeostasis of keratinocyte proliferation and differentiation as seen in psoriatic skin, resulting in multiple changes in the skin and the loss of its radiance.

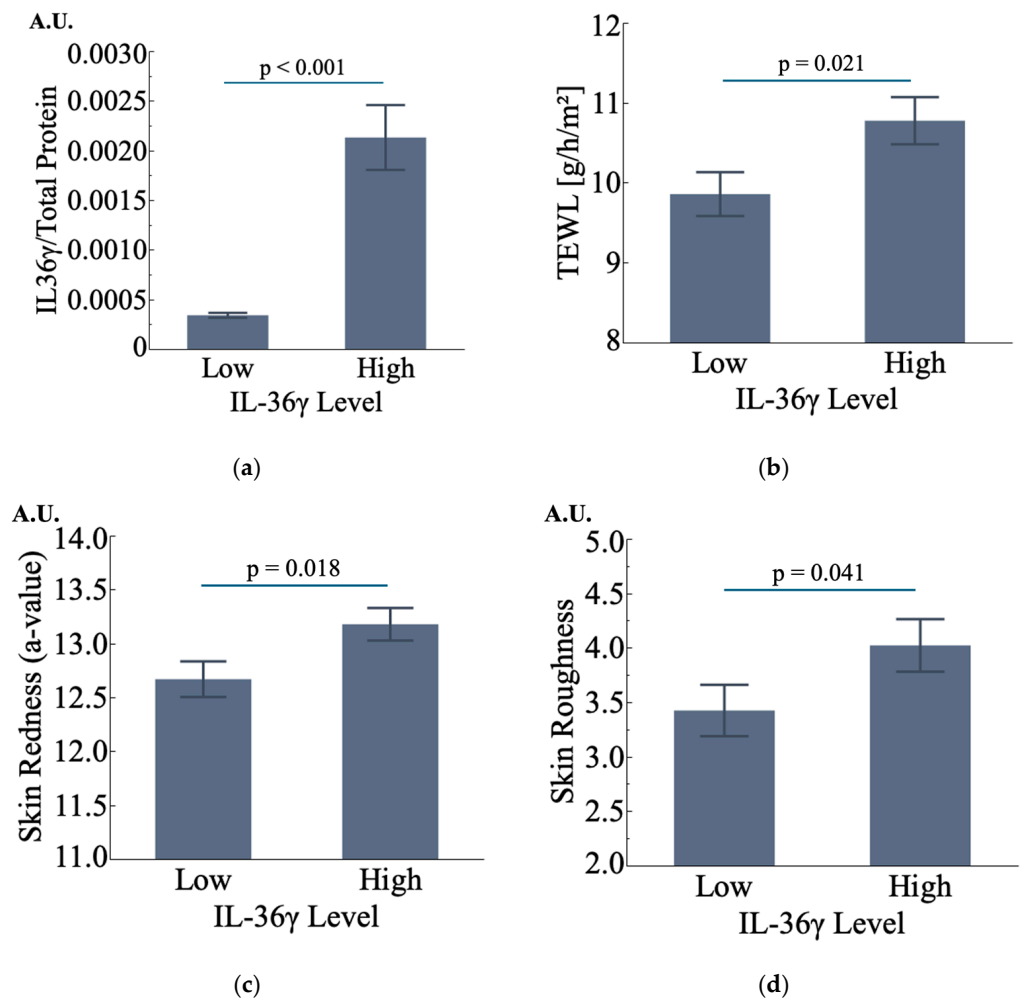


**Figure 8.** Skin differences by IL-36 $\gamma$  Levels. The population was grouped by the median of IL-36 $\gamma$  levels. (a) Confirmatory figure to show the difference in IL-36 $\gamma$  in both groups, (b) TEWL, (c) Skin redness, and (d) Skin roughness.

### 3.5. Effect of Skincare Materials on Identified Biomarkers

#### 3.5.1. Effect on IL-36 $\gamma$

To investigate the effect of skincare materials on IL-36 $\gamma$  expression, we treated monolayers of normal human epidermal keratinocytes (HEK<sub>n</sub>) with GFF, bisabolol, or batyl alcohol for 24 h. The treated cells were then assayed using ELISA to measure IL-36 $\gamma$  levels. The results showed that 5.0% GFF and 0.25% batyl alcohol significantly reduced the expression of IL-36 $\gamma$  compared with that upon control treatment with DMSO, while bisabolol showed no effect (Figure 9).

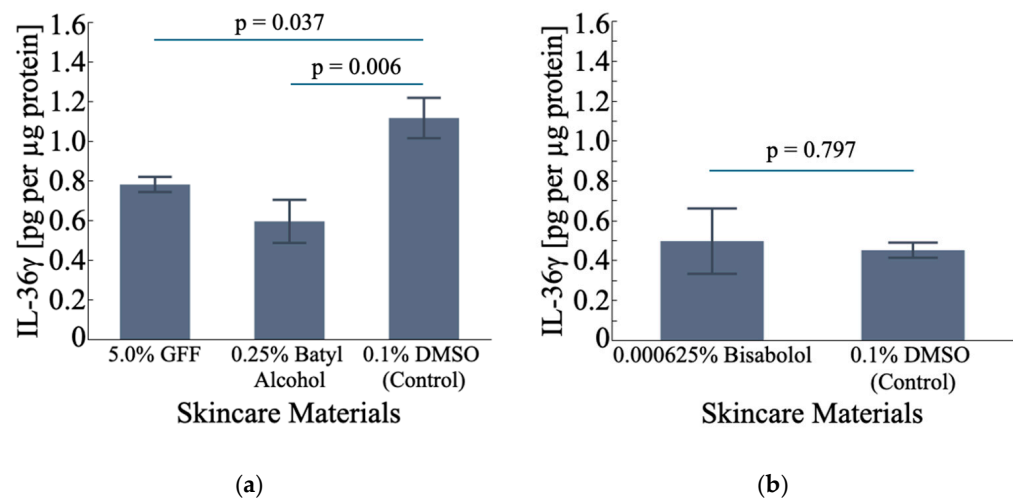


**Figure 9.** Effect of skincare materials on IL-36γ expression. (a) Effect of 5.0% GFF or 0.25% batyl alcohol. (b) Effect of 0.000625% bisabolol. HEK293T cells at 70% confluence were treated with GFF, batyl alcohol, or bisabolol for 24 h. Total protein was extracted from the cells, quantified, and equal amounts of protein were assayed by ELISA.

### 3.5.2. Effect on CDH1

Similarly to the analysis of IL-36γ, to investigate the effect of skincare materials on CDH1 expression, HEK293T cells were treated for 24 h with GFF, bisabolol, or batyl alcohol. The treated cells were then assayed using ELISA to measure CDH1 levels. The results showed that 5.0% GFF significantly increased CDH1 expression compared with the DMSO control, while bisabolol and batyl alcohol had no effect (Figure 10).

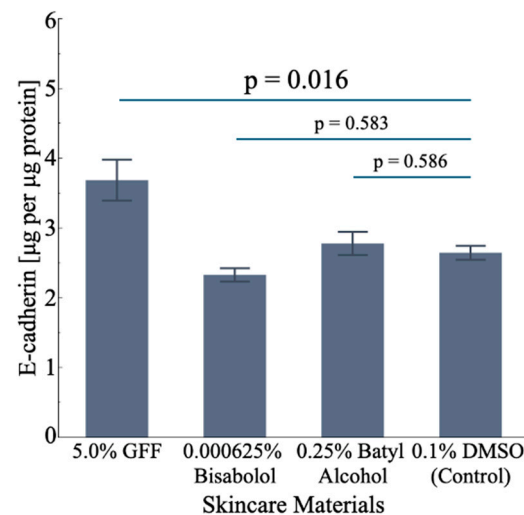


**Figure 10.** Effect of skincare materials on CDH1. HEK293T cells at 70% confluence were treated with 5.0% GFF, 0.000625% bisabolol, or 0.25% batyl alcohol for 24 h. Total protein was extracted from the cells, quantified, and equal amounts of protein were assayed by ELISA.

### 3.5.3. Effect on FLG

To investigate the effect of skincare materials on FLG expression, a skin equivalent 3D model was treated for 5 days with GFF, bisabolol, or batyl alcohol. This model was then immunofluorescently stained for FLG. The stained FLG was quantified using image analysis. The results showed that 10% GFF and 0.005% bisabolol upregulated FLG production in the skin (Figure 11). Histological analysis showed not only that the location of FLG production became slightly deeper in the skin, but also that the amount of FLG clearly increased throughout the upper layers, with the effect extending well into the stratum corneum

layer where post-processing FLG peptides remained (Figure 11). Quantification by image analysis showed that these differences were statistically significant compared with the DMSO control (Figure 12). Meanwhile, batyl alcohol was not confirmed to have any effect on FLG.

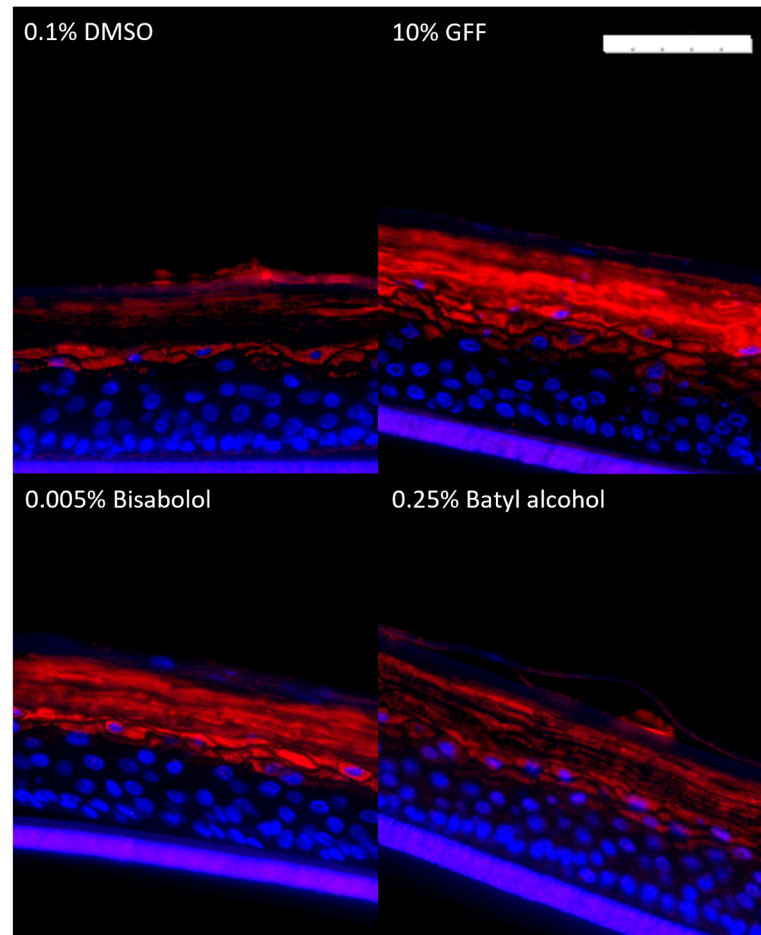


**Figure 11.** FLG staining (red) upon skincare materials treatment. The 3D skin equivalent cultures were topically treated for 5 days with 0.1% DMSO, 10% GFF, 0.005% bisabolol, or 0.25% batyl alcohol, and then immunofluorescently stained for FLG. Scale bar represents 100  $\mu\text{m}$ .

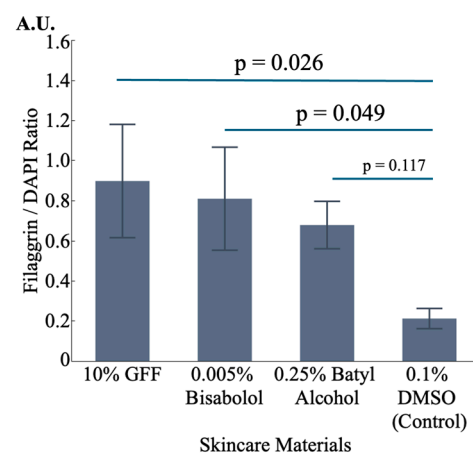


**Figure 12.** Effect of skincare materials on FLG. Quantification was conducted by FLG staining area (red) relative to DAPI nuclear staining area (blue) in Figure 11.

#### 4. Discussion

Our study aimed to investigate the mechanisms underlying dullness or radiance of the skin among young females (age  $\leq 35$ ) beyond the chronological aging. One of the frequently observed situations when skin dullness appears unrelated to chronological aging is lack of sleep. We hypothesized that cellular or molecular level changes in the skin may be involved in the formation of dull skin in this condition other than skin pigmentation. Therefore, as an exploratory step in our research, we utilized MPT and observed differences between radiant and dull skin at the cellular level. To dig deeper, biochemical composition analysis was conducted using a tape-stripping method. These measurements revealed alterations of keratinocyte cellular structures and potential biomarkers of dull skin, which are IL-36 $\gamma$ , CDH1, and FLG.

The MPT measurement results showed that the stratum granulosum layer, where nucleated keratinocytes and fully cornified denucleated cells were collocated, was thicker in dull skin than in radiant skin (Figure 4). Furthermore, in deeper layers of the epidermis (considered as the stratum spinosum and/or partially basal layer), fewer nuclei were observed in dull skin than in radiant skin (Figure 5). These changes are similarly observed in psoriatic skin that exhibits inappropriate keratinocyte differentiation, including malfunctioning of the cornified layers [31,32]. Shutova et al. reported that the expression of adherens junction proteins such as CDH1 is decreased in 2D human keratinocyte models stimulated with inflammatory cytokines such as IL-36 $\gamma$ ; as a result, gaps form between the cells [33]. These link the findings from our biophotonic observations with biochemical analysis results, and we hypothesize that these psoriasis-like cellular condition may be involved in the formation of dull skin.

IL-36 $\gamma$  plays a significant role in the pathogenesis of various inflammatory skin conditions or diseases, especially notable in psoriasis [34–36], where it has three main effects: inhibiting keratinocyte differentiation, promoting keratinocyte proliferation, and priming an overactive immune response [37,38]. Psoriasis patients typically exhibit elevated IL-36 $\gamma$  with various skin issues that are found with dull skin (Figure 6a) [39,40]. Psoriasis is recognized to downregulate the production of proteins such as FLG [41,42]. FLG and its metabolites are critical to the health and appearance of the skin [43]. For example, significant deficiency of FLG is associated with atopic dermatitis (AD) [41] and AD skin is characterized by roughness and a lack of FLG, which is typically broken down into amino acids during the keratinization process and is rarely found in healthy stratum corneum [43]. If IL-36 $\gamma$  is elevated in dull skin, it is plausible that FLG metabolites may also be decreased in dull skin. In our analysis, we observed reductions in PCA and UCA, major natural moisturizing factors (NMFs) derived from FLG, along with an increase in IL-36 $\gamma$ , in the dull skin group. This supports our hypothesis.

CDH1 is known as an adhesive molecule in adherens junctions in keratinocytes and to support proper skin differentiation. CDH1 expression was also found to be decreased in psoriasis [44,45]. In our study, CDH1 was found to be downregulated in individuals with dull skin compared with the level in those with radiant skin (Figure 6b). As CDH1 functions to connect cells, the reduction of CDH1 in dull skin explains the insights from biophotonic epidermal cell observations, where the cells from dull skin were found to be less densely packed. In addition, these molecular differences were accompanied by higher TEWL in individuals with higher IL-36 $\gamma$ , indicating that skin barrier function could be impaired when IL-36 $\gamma$  production is upregulated in the skin.

The decreased levels of FLG and CDH1 both contribute to the impairment of skin barrier function, leading to dehydrated skin, and could cause multiple issues with the appearance of the skin such as roughness. Based on these findings, it can be inferred that the presence of IL-36 $\gamma$  may lead to the deterioration of key signature proteins of skin health, such as FLG and CDH1, ultimately resulting in dull skin.

IL-36 $\gamma$  is an inflammatory cytokine that is a member of the IL-1 family, which is normally only expressed in significant amounts in wounded or infected skin [46,47]. It is important to note that the protein expression of IL-36 $\gamma$  in psoriasis patients examined

through tape stripping was found to be much higher than we describe here, at approximately 600–700 pg per microgram of total protein on average [32]. The levels of IL-36 $\gamma$  and the magnitude of TEWL increment observed in the subjects in this study were within the normal range for healthy skin, and none of the subjects displayed clear symptoms of psoriasis. Therefore, while dull skin appears to share some cellular and molecular characteristics with psoriasis, dullness does not signify the presence of diseased skin. Instead, the findings suggest that individuals with dull skin may be experiencing a mild inflammatory, psoriasis-like condition in their skin. Nonetheless, given the multiple downstream effects of IL-36 $\gamma$ , it is reasonable to assert that any expression below the healthy threshold could induce mild dysfunctions of keratinocyte maturation and skin barrier function in individuals, and this skin state might be recognized as duller skin.

The cellular structure and molecular composition of the skin could play significant roles in determining the appearance of skin radiance or dullness. Skin radiance and dullness are strongly influenced by skin chromophores such as melanin, hemoglobin, and bilirubin, as these chromophores absorb light and reduce the amount of light reflected from the skin surface. When light is irradiated onto the skin, a small proportion of it (4–7%) is reflected at the surface, while the majority penetrates into the skin [48]. The incident light is not only absorbed by skin chromophores but also interacts with cellular structures, such as the nucleus and cytoplasmic structures like mitochondria [49]. Among these interactions, scattering from the nucleus plays a significant role in internal scattering [50]. This type of scattering, known as Mie scattering, occurs when the scattered particles are similar in size to the wavelength of light. Mammalian cell nuclei typically have diameters ranging from 3 to 10  $\mu\text{m}$ , which is close to the wavelength of visible light (400 to 700 nm) [51]. The light scattered from one cell nucleus continues to propagate inside the skin, hitting other nuclei and undergoing further scattering. This cascading scattering process, called multiple scattering, causes the light to diffuse throughout the living tissue, resulting in the observation of scattered light as it subsequently exits the skin [49]. In radiant skin, the densely packed keratinocyte nuclei contribute to the formation of skin radiance by enhancing internal scattering in the deeper layers of the epidermis. Additionally, higher levels of FLG and CDH1, which improve the skin barrier and maintain hydration, contribute to the translucency of the skin layers [52]. Increased translucency allows more light to penetrate into the skin and facilitates the outward transmission of light from within the skin [52]. Not only biochemically but also optically, restoring the levels of FLG and CDH1 and suppressing IL-36 $\gamma$ , which induces psoriasis-like skin conditions and deteriorates the skin's radiance-producing structure, are potential approaches for improving the appearance of the skin and making its surface more radiant.

In addition, we have assessed the potential of three skincare materials in improving skin dullness. In our investigation, GFF and batyl alcohol demonstrated promising effects in suppressing IL-36 $\gamma$  expression, indicating their potential to mitigate the unique IL-36 $\gamma$ -associated inflammatory condition in dull skin. Additionally, GFF and bisabolol showed the ability to increase FLG production, potentially improving skin differentiation and skin barrier function. GFF also exhibited the ability to upregulate CDH1 expression. Our findings provide valuable insights into these cellular and molecular targets potentially contributing to dull skin. Focusing on these unique targets and restoring proteins associated with healthy skin may offer effective strategies for addressing dullness and improving the appearance of the skin. Further research is needed to explore these mechanisms in more detail and to develop targeted skincare formulations for dull skin.

#### *Limitation of Our Research*

Our findings suggest that the tested skincare materials may be effective at improving dullness of the skin. However, further validation of these findings via human study is warranted.

## 5. Conclusions

Underneath dull skin of younger females (age  $\leq 35$ ), various cellular and molecular alterations are exhibited such as a thicker stratum granulosum, less densely packed keratinocytes in deeper layers of epidermis, and elevation of interleukin-36 $\gamma$  and decline of E-cadherin and filaggrin. These alterations indicate that psoriatic skin conditions may be involved in the formation of skin dullness. Our results showed that galactomyces fermentation filtrate as skincare material is effective in suppressing interleukin-36 $\gamma$  while increasing E-cadherin and filaggrin levels, and batyl alcohol and bisabolol have an effect on interleukin-36 $\gamma$  and filaggrin, respectively. However, further validation through human study is necessary to confirm the efficacy of these materials.

**Author Contributions:** Conceptualization, A.M., T.O. and T.H.; methodology, A.M., T.O., Y.X., A.E., L.L., C.P.B., J.I.B. and D.S.; software, T.O. and Y.X.; validation, T.O. and Y.X.; formal analysis, A.M. and A.E.; investigation, A.M., T.O., Y.X. and G.D.; resources, H.N.; data curation, A.M. and H.N.; writing—original draft preparation, A.M., T.O., Y.X., A.E., L.L., W.Z., C.P.B. and T.H.; writing—review and editing, A.M. and T.H.; visualization, A.M.; supervision, A.M., W.Z., B.J., J.W. and T.H.; funding acquisition, A.M., T.O. and Y.X. All authors have read and agreed to the published version of the manuscript.

**Funding:** This research received no external funding.

**Institutional Review Board Statement:** Our human studies were conducted in accordance with the Declaration of Helsinki and approved by the Ethical Review Board of Interface Inc., Akita, Japan (IRB number: 21000027) and the Ethics Committee of Cosmetics Technology Center, Chinese Academy of Inspection and Quarantine, Beijing, China (IRB number: 2023-008-DY-192).

**Informed Consent Statement:** Informed consent was obtained from all subjects involved in the study. Written informed consent has been obtained from the patients to publish this paper.

**Data Availability Statement:** The data are available from the corresponding author upon reasonable request.

**Acknowledgments:** We would like to thank HiuFung Lau and MinNing Yee from the Procter & Gamble Singapore Innovation Center for their technical support regarding tape-stripping capabilities. We also extend our gratitude to Sheldon Xu and Jiang Han from the Procter & Gamble Beijing Innovation Center for their assistance with the skin study in China and for collecting data with MPT and DTIS. Additionally, we would like to thank the recent AI technology, ChatPG based on ChatGPT-3.0, for helping to enhance the quality of English in our manuscript.

**Conflicts of Interest:** This research is funded by Procter & Gamble. A.M., T.O., Y.X., A.E., L.L., W.Z., C.P.B., D.S., H.N., J.I.B., B.J., G.D., and T.H. are employees of Procter & Gamble. The remaining authors declare that the research was conducted in the absence of any commercial or financial relationships that could be construed as a potential conflict of interest.

## References

1. Matsubara, A.; Liang, Z.; Sato, Y.; Uchikawa, K. Analysis of Human Perception of Facial Skin Radiance by Means of Image 612 Histogram Parameters of Surface and Subsurface Reflections from the Skin. *Skin Res. Technol.* **2012**, *18*, 265–271. [[CrossRef](#)] [[PubMed](#)]
2. Jeudy, A.; Ecarnot, V.; Humbert, P. Measurement of Skin Radiance. In *Agache's Measuring the Skin*; Humbert, P., Maibach, H., Fanian, F., Agache, P., Eds.; Springer: Cham, Switzerland, 2015. [[CrossRef](#)]
3. Martschin, C.; Bahhady, R.; Li, J.; Loureiro, W.; Mansour, W.; Metelitsa, A.; Minocha, K.; Somenek, M.; Taghetchian, K.; Tienthavorn, T. Development and Validation of a Novel Holistic Skin Quality Assessment Scale. *J. Cosmet. Dermatol.* **2024**. [[CrossRef](#)] [[PubMed](#)]
4. Fink, B.; Matts, P.J.; Brauckmann, C.; Gundlach, S. The effect of skin surface topography and skin colouration cues on perception of male facial age, health and attractiveness. *Int. J. Cosmet. Sci.* **2018**, *40*, 193–198. [[CrossRef](#)] [[PubMed](#)]
5. Ikeda, H.; Saheki, Y.; Sakano, Y.; Wada, A.; Ando, H.; Tagai, K. Facial radiance influences facial attractiveness and affective impressions of faces. *Int. J. Cosmet. Sci.* **2021**, *43*, 144–157. [[CrossRef](#)]
6. da Silva Souza, I.D.; Lampe, L.; Winn, D. New topical tranexamic acid derivative for the improvement of hyperpigmentation and inflammation in the sun-damaged skin. *J. Cosmet. Dermatol.* **2021**, *20*, 561–565. [[CrossRef](#)]

7. Tarshish, E.; Hermoni, K. Beauty from within: Improvement of skin health and appearance with Lycomato a tomato-derived oral supplement. *J. Cosmet. Dermatol.* **2023**, *22*, 1786–1798. [[CrossRef](#)]
8. de Rigal, J.; Des Mazis, I.; Diridollou, S.; Querleux, B.; Yang, G.; Leroy, F.; Barbosa, V.H. The effect of age on skin color and color heterogeneity in four ethnic groups. *Skin Res. Technol.* **2010**, *16*, 168–178. [[CrossRef](#)]
9. Kaneko, O.; Tsukada, H.; Ishikawa, Y.; Kawaguchi, Y. Measuring Apparent Darkening of the Skin (First Report): Factors Inherent in Light Reflected from the Skin. *J. Soc. Cosmet. Chem. Jpn.* **1997**, *31*, 44–51. [[CrossRef](#)]
10. Kaneko, O.; Kawaguchi, Y.; Ishikawa, Y.; Inagaki, K. Measuring Apparent Darkening of the Skin (Second Report): Relationship between Age-associated Changes in Physical Properties of the Skin and Apparent Darkening. *J. Soc. Cosmet. Chem. Jpn.* **1997**, *31*, 429–438. [[CrossRef](#)]
11. Petitjean, A.; Sainthillier, J.M.; Mac-Mary, S.; Muret, P.; Closs, B.; Gharbi, T.; Humbert, P. Skin Radiance: How to Quantify? Validation of an Optical Method. *Skin Res. Technol.* **2007**, *13*, 2–8. [[CrossRef](#)]
12. Nurani, A.M.; Kikuchi, K.; Iino, M.; Shirasugi, Y.; Sonoki, A.; Fujimura, T.; Hasegawa, K.; Shibata, T. Development of a Method for Evaluating Skin Dullness: A Mathematical Model Explaining Dullness by the Color, Optical Properties, and Microtopography of the Skin. *Skin Res. Technol.* **2023**, *29*, e13407. [[CrossRef](#)] [[PubMed](#)]
13. Lua, B.L.; Robic, J. Yellowness in skin complexion: Analysis of self-perception of women in China evaluated against clinical parameters of yellowness. *Skin Res. Technol.* **2024**, *30*, e13831. [[CrossRef](#)] [[PubMed](#)]
14. Kawabata, K.; Yoshikawa, H.; Saruwatari, K.; Akazawa, Y.; Inoue, T.; Kuze, T.; Sayo, T.; Uchida, N.; Sugiyama, Y. The presence of N( $\epsilon$ )-(Carboxymethyl) lysine in the human epidermis. *Biochim. Biophys. Acta* **2011**, *1814*, 1246–1252. [[CrossRef](#)] [[PubMed](#)]
15. Laughlin, T.; Tan, Y.; Jarrold, B.; Chen, J.; Li, L.; Fang, B.; Zhao, W.; Tamura, M.; Matsubara, A.; Deng, G.; et al. Autophagy activators stimulate the removal of advanced glycation end products in human keratinocytes. *J. Eur. Acad. Dermatol. Venereol.* **2020**, *34* (Suppl. 3), 12–18. [[CrossRef](#)]
16. Kim, M.A.; Kim, E.J.; Kang, B.Y.; Lee, H.K. The Effects of Sleep Deprivation on the Biophysical Properties of Facial Skin. *J. Cosmet. Dermatol. Sci. Appl.* **2017**, *7*, 34–47. [[CrossRef](#)]
17. Anwar, S.S.; Apolinar, M.A.; Ma, L. Perception, understanding, and association between psychological stress and skin aging: Quantitative surveys of Asian women aged 18–34 years, dermatologists, and psychologists in China and Japan. *J. Cosmet. Dermatol.* **2023**, *22*, 2297–2307. [[CrossRef](#)]
18. Irwin, M.R.; Olmstead, R.; Carrol, J.E. Sleep Disturbance, Sleep Duration, and Inflammation: A Systematic Review and Meta-Analysis of Cohort Studies and Experimental Sleep Deprivation. *Biol. Psychiatry* **2016**, *80*, 40–52. [[CrossRef](#)]
19. Irwin, M.R.; Wang, M.; Campomayor, C.O.; Collado-Hidalgo, A.; Cole, S. Sleep Deprivation and Activation of Morning Levels of Cellular and Genomic Markers of Inflammation. *Arch. Intern. Med.* **2006**, *166*, 1756–1762. [[CrossRef](#)]
20. Miyamoto, K.; Kudoh, H. Quantification and visualization of cellular NAD(P)H in young and aged female facial skin with in vivo two-photon tomography. *Br. J. Dermatol.* **2013**, *169* (Suppl. 2), 25–31. [[CrossRef](#)]
21. Marsh, B.P.; Chada, N.; Sanganna Gari, R.R.; Sigdel, K.P.; King, G.M. The Hessian Blob Algorithm: Precise Particle Detection in Atomic Force Microscopy Imagery. *Sci. Rep.* **2018**, *8*, 978. [[CrossRef](#)]
22. Holcomb, J.D. Helium plasma dermal resurfacing: VISIA CR assessment of facial spots, pores, and wrinkles-Preliminary findings. *J. Cosmet. Dermatol.* **2021**, *20*, 1668–1678. [[CrossRef](#)] [[PubMed](#)]
23. Miyamoto, K.; Takiwaki, H.; Hillebrand, G.G.; Arase, S. Development of a Digital Imaging System for Objective Measurement of Hyperpigmented Spots on the Face. *Skin Res. Technol.* **2002**, *8*, 227–235. [[CrossRef](#)] [[PubMed](#)]
24. Dissanayake, B.; Miyamoto, K.; Purwar, A.; Chye, R.; Matsubara, A. New Image Analysis Tool for Facial Pore Characterization and Assessment. *Skin Res. Technol.* **2019**, *25*, 631–638. [[CrossRef](#)] [[PubMed](#)]
25. Miyamoto, K.; Dissanayake, B.; Omotezako, T.; Takemura, M.; Tsuji, G.; Furue, M. Daily Fluctuation of Facial Pore Area, Roughness and Redness among Young Japanese Women; Beneficial Effects of Galactomyces Ferment Filtrate Containing Antioxidative Skin Care Formula. *J. Clin. Med.* **2021**, *5*, 10–2502. [[CrossRef](#)]
26. Omotezako, T.; Neo, E.; Zhu, H.; Ehrman, M. Disordered spatial pattern of redness signal on facial skin and visual perception of health, stress, and hidden aging. *Skin Res. Technol.* **2024**, *30*, e13628. [[CrossRef](#)]
27. Omotezako, T.; Zhao, W.; Rodrigues, M.; Ehrman, M.; Deng, D.; Lau, H.; Hakozaiki, T. Skin inflammatory signatures, as measured by disordered spatial redness patterns, predict current and future skin ageing attributes. *Exp. Dermatol.* **2024**, *33*, e15163. [[CrossRef](#)]
28. De Paepe, K.; Houben, E.; Adam, R.; Wiesemann, F.; Rogiers, V. Validation of the VapoMeter, a closed unventilated chamber system to assess transepidermal water loss vs. the open chamber Tewameter. *Skin Res. Technol.* **2005**, *11*, 61–69. [[CrossRef](#)]
29. Kaleja, P.; Emmert, H.; Gerstel, U.; Weidinger, S.; Tholey, A. Evaluation and improvement of protein extraction methods for analysis of skin proteome by noninvasive tape stripping. *J. Proteomics.* **2020**, *15*, 217–103678. [[CrossRef](#)]
30. Hakozaiki, T.; Wang, J.; Laughlin, T.; Jarrold, B.; Zhao, W.; Furue, M. Role of interleukin-6 and endothelin-1 receptors in enhanced melanocyte dendricity of facial spots and suppression of their ligands by niacinamide and tranexamic acid. *J. Eur. Acad. Dermatol. Venereol.* **2023**, *38* (Suppl. 2), 3–10. [[CrossRef](#)]
31. Ghadially, R.; Reed, J.T.; Elias, P.M. Stratum Corneum Structure and Function Correlates with Phenotype in Psoriasis. *J. Investig. Dermatol.* **1996**, *107*, 558–564. [[CrossRef](#)]
32. Wolf, R.; Orion, E.; Ruocco, E.; Ruocco, V. Abnormal Epidermal Barrier in the Pathogenesis of Psoriasis. *Clin. Dermatol.* **2012**, *30*, 323–328. [[CrossRef](#)] [[PubMed](#)]

33. Shutova, M.S.; Borowczyk, J.; Russo, B.; Sellami, S.; Drukala, J.; Wolnicki, M.; Brembilla, N.C.; Kaya, G.; Ivanov, A.I.; Boehncke, W.-H. Inflammation Modulates Intercellular Adhesion and Mechanotransduction in Human Epidermis via ROCK2. *iScience* **2023**, *26*, 106195. [[CrossRef](#)] [[PubMed](#)]
34. Sachen, K.L.; Greving, C.N.A.; Towne, J.E. Role of IL-36 Cytokines in Psoriasis and Other Inflammatory Skin Conditions. *Cytokine* **2022**, *156*, 155897. [[CrossRef](#)] [[PubMed](#)]
35. D'Erme, A.M.; Wilsmann-Theis, D.; Wagenpfeil, J.; Hölzel, M.; Ferring-Schmitt, S.; Sternberg, S.; Wittmann, M.; Peters, B.; Bosio, A.; Bieber, T.; et al. IL-36 $\gamma$  (IL-1F9) Is a Biomarker for Psoriasis Skin Lesions. *J. Investig. Dermatol.* **2014**, *135*, 1025–1032. [[CrossRef](#)]
36. Macleod, T.; Ainscough, J.S.; Hesse, C.; Konzok, S.; Braun, A.; Buhl, A.; Wenzel, J.; Bowyer, P.; Terao, Y.; Herrick, S.; et al. The Proinflammatory Cytokine IL-36 $\gamma$  Is a Global Discriminator of Harmless Microbes and Invasive Pathogens within Epithelial Tissues. *Cell Rep.* **2020**, *33*, 108515. [[CrossRef](#)]
37. Buhl, A.; Wenzel, J. Interleukin-36 in Infectious and Inflammatory Skin Diseases. *Front. Immunol.* **2019**, *10*, 1162. [[CrossRef](#)]
38. Queen, D.; Ediriweera, C.; Liu, L. Function and Regulation of IL-36 Signaling in Inflammatory Diseases and Cancer Development. *Front. Cell Dev. Biol.* **2019**, *7*, 317. [[CrossRef](#)]
39. Rendon, A.; Schäkel, K. Psoriasis Pathogenesis and Treatment. *Int. J. Mol. Sci.* **2019**, *20*, 1475. [[CrossRef](#)]
40. Montero-Vilchez, T.; Segura-Fernández-Nogueras, M.V.; Pérez-Rodríguez, I.; Soler-Gongora, M.; Martínez-Lopez, A.; Fernández-González, A.; Molina-Leyva, A.; Arias-Santiago, S. Skin Barrier Function in Psoriasis and Atopic Dermatitis: Transepidermal Water Loss and Temperature as Useful Tools to Assess Disease Severity. *J. Clin. Med.* **2021**, *10*, 359. [[CrossRef](#)]
41. Hu, Z.; Xiong, Z.; Xu, X.; Li, F.; Lu, L.; Li, W.; Su, J.; Liu, Y.; Liu, D.; Xie, Z.; et al. Loss-of-Function Mutations in Filaggrin Gene Associate with Psoriasis Vulgaris in Chinese Population. *Hum. Genet.* **2012**, *131*, 1269–1274. [[CrossRef](#)]
42. Jensen, P.; Skov, L. Filaggrin in Psoriasis. In *Filaggrin*; Thyssen, J., Maibach, H., Eds.; Springer: Berlin, Heidelberg, 2014. [[CrossRef](#)]
43. Harding, C.R.; Aho, S.; Bosko, C.A. Filaggrin-Revisited. *Int. J. Cosmet. Sci.* **2013**, *35*, 412–423. [[CrossRef](#)] [[PubMed](#)]
44. Wang, W.; Yu, X.; Wu, C.; Jin, H. IL-36 $\gamma$  Inhibits Differentiation and Induces Inflammation of Keratinocyte via Wnt Signaling Pathway in Psoriasis. *Int. J. Med. Sci.* **2017**, *14*, 1002–1007. [[CrossRef](#)] [[PubMed](#)]
45. Chung, E.; Cook, P.W.; Parkos, C.A.; Park, Y.; Pittelkow, M.R.; Coffey, R.J. Amphiregulin Causes Functional Downregulation of Adherens Junctions in Psoriasis. *J. Investig. Dermatol.* **2005**, *124*, 1134–1140. [[CrossRef](#)] [[PubMed](#)]
46. Berekméri, A.; Latzko, A.; Alase, A.; Macleod, T.; Ainscough, J.S.; Laws, P.; Goodfield, M.; Wright, A.; Helliwell, P.; Edward, S.; et al. Detection of IL-36 $\gamma$  through Noninvasive Tape Stripping Reliably Discriminates Psoriasis from Atopic Eczema. *J. Allergy Clin. Immunol.* **2018**, *142*, 988–991.e4. [[CrossRef](#)] [[PubMed](#)]
47. Madonna, N.; Girolomoni, G.; Dinarello, C.A.; Albanesi, C. The Significance of IL-36 Hyperactivation and IL-36R Targeting in Psoriasis. *Int. J. Mol. Sci.* **2019**, *20*, 3318. [[CrossRef](#)]
48. Gajinov, Z.A.; Matić, M.; Prčić, S.; Đuran, V. Optical Properties of the Human Skin. *Serb. J. Dermatol. Venereol.* **2010**, *2*, 131–136. [[CrossRef](#)]
49. Takehana, S. Vascular Imaging Using Image-Enhanced Endoscopy with Optical-Digital Method and the Application to Portal Hypertension. *Jpn. J. Portal Hypertens.* **2008**, *14*, 156–160. [[CrossRef](#)]
50. Mourant, J.R.; Canpolat, M.; Brocker, C.; Esponda-Ramos, O.; Johnson, T.M.; Matanock, A.; Stetter, K.; Freyer, J.P. Light Scattering from Cells: The Contribution of the Nucleus and the Effects of Proliferative Status. *J. Biomed. Opt.* **2000**, *5*, 131–137. [[CrossRef](#)]
51. Xu, M.; Wu, T.T.; Qu, J.Y. Unified Mie and Fractal Scattering by Cells and Experimental Study on Application in Optical Characterization of Cellular and Subcellular Structures. *J. Biomed. Opt.* **2008**, *13*, 024015. [[CrossRef](#)]
52. Jiang, Z.X.; DeLaCruz, J. Appearance Benefits of Skin Moisturization. *Skin Res. Technol.* **2011**, *17*, 51–55. [[CrossRef](#)]

**Disclaimer/Publisher's Note:** The statements, opinions and data contained in all publications are solely those of the individual author(s) and contributor(s) and not of MDPI and/or the editor(s). MDPI and/or the editor(s) disclaim responsibility for any injury to people or property resulting from any ideas, methods, instructions or products referred to in the content.